Title

A Phospholipase C-γ1–Independent, RasGRP1-ERK–Dependent Pathway Drives Lymphoproliferative Disease in Linker for Activation of T Cells–Y136F Mutant Mice

Permalink

https://escholarship.org/uc/item/031882nj

Journal

The Journal of Immunology, 190(1)

ISSN

0022-1767

Authors

Kortum, Robert L
Rouquette-Jazdanian, Alexandre K
Miyaji, Michihiko
et al.

Publication Date

2013

DOI

10.4049/jimmunol.1201458

Peer reviewed

A PLC-γ1-independent, RasGRP1-ERK dependent pathway drives lymphoproliferative disease in LAT-Y136F mutant mice

Robert L. Kortum[*], **Alexandre K. Rouquette-Jazdanian**[*], **Michihiko Miyaji**[*,†], **Robert K. Merrill**[*], **Evan Markegard**[‡], **John M. Pinski**[*], **Amelia Wesselink**[*], **Nandan N. Nath**[*], **Clayton P. Alexander**[*], **Wenmei Li**[*], **Noemi Kedei**[§], **Jeroen P. Roose**[‡], **Peter M. Blumberg**[§], **Lawrence E. Samelson**[*], and **Connie L. Sommers**[*,¶]

[*]Laboratory of Cellular and Molecular Biology, National Cancer Institute, National Institutes of Health, Bethesda, MD 20892, USA

[§]Laboratory of Cancer Biology and Genetics, National Cancer Institute, National Institutes of Health, Bethesda, MD 20892, USA

[‡]Department of Anatomy, University of California San Francisco, San Francisco, CA 94143, USA

Abstract

Mice expressing a germline mutation in the PLC-γ1 binding site of LAT (linker for activation of T cells) show progressive lymphoproliferation and ultimately die at 4–6 months of age. The hyper-activated T cells in these mice show defective TCR-induced calcium flux, but enhanced Ras/ERK activation that is critical for disease progression. Despite the loss of LAT-dependent PLC-γ1 binding and activation, genetic analysis revealed RasGRP1, and not Sos1 or Sos2, to be the major RasGEF responsible for ERK activation and the lymphoproliferative phenotype in these mice. Analysis of isolated CD4^{+} T cells from LAT-Y136F mice showed altered proximal TCR-dependent kinase signaling, which activated a Zap70- and LAT-independent pathway. Moreover, LAT-Y136F T cells showed ERK activation that was dependent on Lck and/or Fyn, PKCθ, and RasGRP1. These data demonstrate a novel route to Ras activation *in vivo* in a pathological setting.

Introduction

Engagement of the TCR by a peptide-MHC complex ligand triggers tyrosine phosphorylation of ITAMs on the TCRζ and CD3 chains by the Src family kinases (SFKs) Lck and Fyn, allowing for the recruitment and activation of the tyrosine kinase ZAP70 (1). ZAP70 then rapidly phosphorylates the membrane-bound adaptor linker for activation of T cells (LAT) on five of nine conserved tyrosines in its C-terminal tail, four of which (Y136, Y175, Y195, Y235) seem critical for the adaptor function of LAT (2). These phosphorylated tyrosines then act as docking sites for SH2 domain-containing proteins, allowing for the recruitment of numerous multi-protein complexes to LAT. Recruitment of these signaling complexes to the membrane by LAT activates multiple intracellular signaling pathways controlling both T cell development and effector functions (3).

Activation of the small G protein Ras is central to numerous physiologic and pathologic conditions. In T cells, phosphorylated LAT associates with two molecular complexes that regulate Ras activation: PLC-γ1/GADS/SLP-76 and Grb2/Sos (4). Phospholipase C-γ1

¶Correspondence: Connie L. Sommers, Laboratory of Cellular and Molecular Biology and Center for Cancer Research, National Cancer Institute National Institutes of Health 37 Convent Drive Bldg. 37, Room 2064 Bethesda, MD 20892-4256 301-496-8910 301-496-8479 (fax) sommersc@helix.nih.gov.
†Present address, First Department of Internal Medicine, Kansai Medical University, Moriguchi City, Osaka 570-8506, Japan.

(PLC-γ1) interacts with LAT pY136, and stabilization of this interaction by the adaptors GADS (binds LAT pY175 and pY195) and SLP-76 (binds GADS and PLC-γ1) allows for phosphorylation of PLC-γ1 on residues critical for its activation (5). Activated PLC-γ1 then cleaves PIP_2 generating IP_3, which stimulates release of intracellular calcium stores, and diacylglycerol (DAG). DAG activates the Ras guanine exchange factor (RasGEF) RasGRP1 both directly by binding its C1 domain, and indirectly by activating novel protein kinase C (PKC) isoforms, which phosphorylates RasGRP1 on T184 and increase its RasGEF activity (6).

The RasGEFs Sos1 and Sos2 are constitutively associated with the adaptor Grb2 and are recruited to the membrane where they have basal RasGEF activity via Grb2-LAT interactions (Grb2 binds LAT pY175, pY195, and pY235) (5). Furthermore, Sos proteins contain an allosteric Ras-GTP binding site that, when engaged, markedly enhances their RasGEF activity (7). Ras-GTP binding to Sos allows for the engagement of a positive feedback loop between Ras and Sos, primed by either RasGRP1 or basal Sos activity, which can be employed when high levels of Ras activation are required (8, 9). Generation of activated Ras then activates multiple downstream pathways, including the Raf/MEK/ERK kinase cascade, to drive both T cell development and effector functions (10, 11).

Studies assessing the role of LAT *in vivo* using mouse models have revealed that LAT is essential for T cell development. LAT deletion or a knock-in mutation of the distal 4 tyrosine residues of LAT (LAT-4YF) led to a complete block in pre-TCR-driven developmental signals and failure of T cell precursors to develop beyond the CD4⁻CD8⁻(DN) stage (12, 13). Knock-in mutations of either Y175/195/235F (3YF) or Y136F (1YF) in LAT caused a DN thymocyte block in young mice (14–16). However, as these mice aged they developed a marked post-thymic expansion of either γδ or αβ T cells, respectively (14–16) leading to massive splenomegaly, lymph node enlargement, and lymphocyte infiltration of non-lymphoid organs. The hyper-proliferative αβ T cells found in LAT-Y136F mice show a T_H2 CD4⁺ activated/memory phenotype (CD44^hiCD62L^lo) indicative of prior stimulation (14, 16), and require signals from both MHC class II and CD28 for their development (17). Isolated CD4⁺ T cells from LAT-Y136F mice showed defective TCR-dependent PLC-γ1 phosphorylation and Ca⁺⁺ flux (16) consistent with the mutation of the Y136 PLC-γ1 binding site on LAT. However, these mutant CD4⁺ T cells showed a hyper-activation of ERK kinase signaling that helped drive disease progression (18). Genetic analysis showed that this altered ERK activation was dependent, in part, on a novel Bam32-ERK signaling pathway, as Bam32 deletion led to a reduction in ERK signaling and delayed disease progression in LAT-Y136F mice (18).

We sought to further characterize the altered signaling pathways that drive ERK hyper-activation, pathologic lymphocyte proliferation, and disease progression in LAT-Y136F mice. We found that the small G protein Ras was hyper-activated in CD4⁺ T cells from LAT-Y136F mice. However, despite lacking PLC-γ1 activation, genetic analysis showed that disease progression and ERK signaling were more dependent on RasGRP1 than on Sos1/2 in LAT-Y136F mice. Analysis of upstream signaling in T cells from these mice revealed Lck and Fyn hyper-activation that did not signal through ZAP70, but activated an unconventional SFK/PKCθ/RasGRP1 pathway to contribute to ERK signaling and disease in this murine model of pathologic lymphocyte proliferation.

Materials and Methods

Mice

RasGRP1⁻/⁻ mice were a gift from James Stone (Univ. of Alberta, CA) (19). Sos2⁻/⁻ mice were generated at LCMB by Eugene Santos (Univ. de Salamanca, ES) (20). Lck-Cre (21)

mice were purchased from Taconic. T cell specific deletion of Sos1 (denoted Sos1(T)$^{-/-}$) was achieved by crossing Sos1$^{f/f}$ mice to mice expressing Lck-CRE (22). Genotyping for LAT-Y136F (16), RasGRP1$^{-/-}$ (19), Sos1(T) $^{-/-}$ (22), Sos2$^{-/-}$ (20), and Cre (21) mice was carried out as detailed in the original publications. All mice were housed at the NIH following guidelines set forth by the NCI-Bethesda Animal Care and Use Committee.

Flow cytometry

Single cell suspensions from thymus of pooled axillary, brachial, and inguinal lymph nodes were stained with the fluorochrome-conjugated monoclonal antibodies described in the text. Flow cytometry was performed using a FACSCalibur and CELLQuest software (BD Biosciences), and data were analyzed using FlowJo software (Tree Star, Inc). All fluorochrome-conjugated antibodies were purchased from BD Biosciences.

Cell purification

For CD4$^+$ LN T cells, total lymphocytes were isolated using the CD4$^+$ T-cell isolation kit (Miltenyi Biotech) according to the manufacturer's instructions. Cells were >90% CD4$^+$ following purification. Purified CD4$^+$ LN cells were then resuspended in pre-warmed RPMI at 1×10^6 cells per 10 μL and allowed to equilibrate to room temperature for 20 min before any additional manipulation.

Cell stimulation, Immunoprecipitation, Ras pull-down, and Western blotting

For stimulation of purified CD4$^+$ lymphocytes, purified cells were resuspended in pre-warmed RPMI at 1×10^6 cells per 10 μL. For each time point, 4×10^6 cells were pre-incubated with 10 μg/mL biotinylated anti-CD3ϵ (145-2C11, BD Biosciences) +/- 10μg/mL biotinylated anti-CD4 (GK1.5, BD Biosciences) for 15 minutes at room temperature. For inhibitor studies, cells were pre-treated for 20 minutes with inhibitor in RPMI prior to incubation with stimulatory antibodies. The inhibitors used included: pan-SFK inhibitor PP2 (23) at 20 μM (Sigma-Aldrich), classical PKC inhibitor Gö6976 (24) at 5 μM (Sigma-Aldrich), pan-PKC inhibitor Gö6983 (25) at 5 μM (Sigma-Aldrich), PKC inhibitor Rottlerin (26) at 20 μM (Sigma-Aldrich), PLC-γ1 inhibitor U73122 (27, 28) at 1 μM (Sigma-Aldrich), inactive enantiomer U73343 (27) at 1 μM (Sigma-Aldrich), phospholipase D (PLD) and phosphatidylcholine-specific PLC (pc-PLC) inhibitor D609 (29) at 300 μM (Alexis Biochemicals), or MEK1/2 inhibitor U0126 (30) at 10 μM (Cell Signaling Technology). All inhibitors were dissolved in DMSO, with a final DMSO concentration of less than 2.5% vol/vol in RPMI. Cells were then washed with RPMI and resuspended at 1×10^6 cells per 10 μL prior to the addition of 40 μL of 2$\times$ streptavidin (20μg/mL final concentration). Stimulation was terminated by the addition of 2$\times$ SDS sample buffer containing 100 mM DTT and boiling for 10 minutes.

For immunoprecipitations (IPs) and Ras-GTP pull-downs (Ras-PDs), 5×10^6 (phospho-pan Src (Y416) IPs) or 10×10^6 (Ras-PDs, TCRζ IPs, Lck IPs, and PCKθ IPs) cells were stimulated as described above or were stimulated without CD4 co-stimulation (Lck and PCKθ IPs). For IPs, samples were lysed for 10 minutes in ice-cold NP-40 lysis buffer (1% NP-40, 10% glycerol, 150 mM NaCl, 50 mM Tris pH 7.5, 1 mM sodium vanadate, protease inhibitor cocktail (Roche)) and pre-cleared using Protein A/G Agarose (Santa Cruz). Lysates were then immunoprepitated using anti-phospho-pan Src Y416 (Cell Signaling, 1:50) or anti-PKCθ (Santa Cruz sc-212, 1:100) for 1 hour. IPs were washed four times in ice-cold lysis buffer without inhibitors. For Ras pull-downs, cells were lysed on ice for 10 minutes in Ras-PD lysis buffer (1% NP-40, 50 mM Tris pH 7.5, 200 mM NaCl, 2.5 mM MgCl$_2$, 1 mM PMSF, protease inhibitor cocktail (Roche)), and spun at 10,000 RPM for 10 minutes. GST-RBD bound to glutathione-sepharose beads was prepared as previously described (31) and used to isolate Ras-GTP from lysates by rotating incubation for one hour at 4°C. Samples

were washed four times in Ras-PD lysis buffer. All samples were boiled in $2\times$ SDS sample buffer containing 100 mM DTT for 10 minutes prior to Western blotting.0

Samples were loaded at 0.5×10^6 cells per lane and separated by 10% SDS-PAGE. The following primary antibodies were used: pMEK1/2 1:1000 Cell Signaling Technology #9154, MEK1/2 1:1000 each #610122 (MEK1) and #610236 (MEK2), pERK1/2 1:2000 Cell Signaling Technology #4370, ERK1/2 1:2000 Cell Signaling Technology #4695, Ras 1:1000 Upstate #05-516, β-actin 1:5000 Sigma-Aldrich #AC-40, pPKCθ (T538) 1:2000 Cell Signaling Technology #9377, PKCθ 1:500 Santa Cruz #sc-212, PKCδ 1:2000 Santa Cruz #sc-937, pRasGRP1 T184 1:2000 (see below), RasGRP1 1:500 Santa Cruz sc-8430, phospho-Tyrosine 4G10 1:4000 Millipore #05-321, phospho-pan Src 1:2000 Cell Signaling Technology (Y416) #2101, Lck 1:2000 Cell Signaling Technology #2752, Fyn 1:1000 each of Santa Cruz #sc-365913 and #sc-73388, Yes 1:1000 Santa Cruz #sc-46674, pZAP70 1:2000 Cell Signaling Technology #2704, ZAP70 1:2000 (32) and TCRζ 1:1000 (33). Blots were incubated with primary antibody at 4°C overnight, and secondary HRP (1:20,000, Millipore) antibodies at RT for 1 hour. ECL was used to visualize protein products (Super Signal West Pico and Super Signal West Femto, Pierce). Protein bands were quantified using ImageJ. Anti-pRasGRP1 T184 mouse monoclonal antibody was generated by immunization with the peptide SRKL-pT-QRIKSNTC together with Eurogentech/Anaspec (Fremont, CA, USA). The column-purified antibody was used at 1:2000 in 5% BSA. Western blots of phosphorylated proteins were stripped and reprobed for their total proteins with the exception of pMEK1/2 and total MEK1/2, as the harsh conditions required to strip the pMEK blots removed the associated MEK proteins as well. For these blots, parallel gels were equally loaded and run simultaneously.

Subcellular Fractionation

Subcellular fractionation was performed as previously described (34). Briefly, cells were washed $1\times$ in ice cold PBS and resuspended in a hypotonic lysis buffer (10 mM Tris-HCl pH 7.5, 5 mM $MgCl_2$, 1 mM EGTA, 100 μM $NaVO_4$). Cells were then passed $30\times$ through a 25 gauge needle and incubated on ice for 10 minutes, and nuclei and unlysed cells were removed by centrifugation at $300\times g$ for 5 minutes. Post-nuclear supernatants were then spun at $100,000\times g$ for 60 minutes, and separated into the soluble (S100) and insoluble (P100) fractions. P100 fractions were resuspended using equal volumes of $2\times$ SDS sample buffer. S100 and P100 fractions were probed with LAT and GAPDH antibodies to ensure >95% enrichment of each fraction (data not shown).

Statistical Analysis

All data are presented as average $+/-$ standard deviation. The significance of the difference between means of two data sets was determined by a two-tailed Student's *t* test. P-values < 0.05 were considered statistically significant. Linear regression analysis of spleen weight data was performed using GraphPad Prism software. For pair-wise comparisons, the slopes of regression analysis were analyzed for differences in disease progression (Table SI). P-values < 0.05 were considered statistically significant.

Results

Mice carrying a germline mutation in the PLC-γ1 binding site of LAT (LAT-Y136F) exhibit a pathologic CD4^{+} T cell lymphoproliferation dependent on the ERK signaling cascade, in part mediated by the adaptor molecule Bam32 (18). We sought to further characterize the signaling pathways that led to lymphoproliferative disease and ERK activation in these mice. Assessment of Ras activation in isolated CD4^{+} T cells from LAT-Y136F mice showed increased basal Ras-GTP levels, which were modestly increased by

mild platebound anti-CD3ε-stimulation, but markedly enhanced by PMA-stimulation (Fig. 1A). To assess whether these pathologic cells show an enhanced capacity to activate Ras, CD4^{+} T cells isolated from WT or LAT-Y136F mice were rested for 6 hours to normalize basal Ras-GTP levels prior to stimulation with PMA +/− ionomycin. CD4^{+} T cells from LAT-Y136F mice showed a marked increase in PMA-stimulated Ras-GTP levels compared to WT controls (Fig. 1B). These data led us to hypothesize that the lymphoproliferative disease observed in LAT-Y136F mice (14, 16) was, at least partially, dependent upon hyper-activation of Ras.

Sos1/2 deletion slows lymphoproliferative disease progression in LAT-Y136F mice

Once phosphorylated, LAT normally associates with two regulators of Ras activation: PLC-γ1, which activates the RasGEF RasGRP1 via DAG, and Grb2, which directly associates with the RasGEFs Sos1 and Sos2 (4). The combined actions of RasGRP1, Sos1 and Sos2 are thought to induce complete Ras activation downstream of the TCR (6, 8, 9, 35). Since TCR-induced LAT-PLC-γ1 association and activation should be abrogated in LAT-Y136F mice (14, 16), we thought that it would be unlikely that RasGRP1 would be activated, and rather that the Ras hyper-activation in LAT-Y136F mice would be due to signaling through Sos1 and/or Sos2.

To directly test this hypothesis, LAT-Y136F mice were crossed to Sos1(T)[−/−] and/or Sos2^{−/−} mice (11, 20, 22) to assess the development of lymphoproliferative disease in the absence of these RasGEFs (Fig. 2 and 3). Deletion of Sos1 or Sos2 alone did not affect the lymphoproliferative disease seen in LAT-Y136F mice as assessed by a time-dependent increase in spleen weight (Fig. 2A–B). Furthermore, assessment of lymph nodes from LAT-Y136F mice by staining with anti-CD4 and anti-CD8 antibodies followed by flow cytometry showed a CD4^{+} T lymphocyte accumulation, which was not altered by Sos1 or Sos2 deletion (Fig. 3A–B). In contrast, combined Sos1/2 deletion significantly slowed LAT-Y136F disease progression, as assessed by either a change in the slope of the regression curve for the time-dependent increases in spleen weight (Fig. 2A and Table SI), or the accumulation of CD4^{+} lymphocytes (Fig. 3A).

LAT-Y136F mice show a substantial early block (DN-to-DP) in thymocyte development (14, 16), and we have previously shown that Sos1 is similarly required for thymocyte development at the DN-to-DP transition (11, 22). Based on these data, one could hypothesize that the reduction in disease burden seen in Sos1/2 DKO mice could simply be due to delayed thymic development and thus a reduced development of CD4^{+} T lymphocytes. To determine whether Sos1 and/or Sos2 deletion altered thymocyte development in LAT-Y136F mice, thymi from young (4-week-old) mice were analyzed to examine thymocyte development at a point where pathologic CD4^{+} T cells are beginning to appear but have not yet overwhelmed the animals (14, 16). Staining with anti-CD4 and anti-CD8 to assess thymocyte development revealed a marked block at the DN-to-DP transition in LAT-Y136F mice (Fig. 4A), with a marked decrease in the number of CD4^{+} CD8^{+} (DP) thymocytes (Fig. 4B) and an increase in the DN/DP ratio (Fig. 4C). While combined Sos1/2 deletion was required to delay lymphoproliferative disease in LAT-Y136F mice (Fig. 2 and 3), deletion of either Sos1 alone or in combination with Sos2 enhanced the DN-to-DP developmental block seen in thymi of young LAT-Y136F mice as assessed by a decrease in the number of DP thymocytes (Fig. 4B) and an increase in the DN/DP ratio (Fig. 4A and C). Since either Sos1 deletion (which did not affect LAT-Y136F lymphoproliferative disease) or combined Sos1/2 deletion (which did delay LAT-Y136F lymphoproliferative disease) showed the same block in thymocyte development, these data show that delaying thymic development alone is insufficient to reduce the disease burden in LAT-Y136F mice.

We next examined whether Sos1/2 deletion directly affected Raf/MEK/ERK kinase cascade activation in CD4^{+} T lymphocytes isolated from LAT-Y136F mice. Combined Sos1/2 deletion diminished, but did not eliminate, both basal and anti-CD3ε + anti-CD4-stimulated MEK and ERK phosphorylation in LAT-Y136F mice (Fig. 5A). These data suggest that while signaling through Sos1/2 contributes to ERK activation in this disease model, other Sos1/2-independent signaling pathways contribute to disease progression in LAT-Y136F mice.

RasGRP1 is the major RasGEF responsible for Ras/ERK activation and lymphoproliferative disease in LAT-Y136F mice

Since Sos1/2 deletion did not eliminate ERK hyper-activation and disease progression in LAT-Y136F mice we addressed the role of RasGRP1 by crossing LAT-Y136F mice to RasGRP1^{−/−} mice (Fig. 2 and 3). Unexpectedly, RasGRP1 deletion led to a major reduction in disease progression compared to LAT-Y136F mice when assessing both the time-dependent increase in spleen weight (Fig. 2A–B) and CD4^{+} lymphocyte accumulation (Fig. 3A–B) seen in LAT-Y136F mice. Direct comparison of LAT-Y136F/Sos1/2 DKO versus LAT-Y136F/RasGRP1^{−/−} mice showed significant differences in CD4^{+} lymphocyte accumulation (Fig. 3A), however the rates of disease progression (Fig. 2A) between these two groups were not quite statistically different (P=0.07, Table SI). These data suggest that deletion of either Sos1/2 or RasGRP1 has a statistically similar effect on the rate of lymphoproliferation in LAT-Y136F mice. Combined deletion of Sos1/2 and RasGRP1 in LAT-Y136F mice (LAT-Y136F/Sos1/2 DKO/RasGRP1^{−/−} mice) eliminated lymphoproliferative disease such that 15 mice examined at >27 weeks of age remained disease free (Fig. 2 and 3). LAT-Y136F/Sos1/2 DKO/RasGRP1^{−/−} mice showed a rate of disease progression that was statistically different than LAT-Y136F/Sos1/2 DKO mice, but not LAT-Y136F/RasGRP1^{−/−} mice (Table SI). These data suggest that RasGRP1 deletion has a more profound effect than Sos1/2 deletion on disease progression in LAT-Y136F mice (Fig. 2A). Furthermore, RasGRP1 deletion almost completely eliminated both basal and anti-CD3ε + anti-CD4-stimulated MEK and ERK phosphorylation in T cells from LAT-Y136F mice (Fig. 5B). These data suggest that a RasGRP1-dependent, PLC-γ1-independent pathway is the major determinant driving both proliferation and ERK activation in LAT-Y136F mice.

An SFK- and PKC-dependent pathway lies upstream of RasGRP1 in CD4^{+} T lymphocytes isolated from LAT-Y136F mice

We next sought to determine which altered upstream signaling pathways were leading to PLC-γ1-independent RasGRP1 activation. Phospho-tyrosine blotting of whole cell lysates from anti-CD3ε + anti-CD4-stimulated LAT-Y136F CD4^{+} T lymphocytes showed a decrease in tyrosine-phosphorylated proteins at 38, 70, and 76 kd (consistent with LAT, ZAP70, and SLP-76, small arrowheads) compared to WT CD4^{+} T lymphocytes (Fig. 6A). However, we observed a significant increase in both basal and stimulated phosphorylation of a doublet at 55 kd (consistent with phosphorylated Src-family kinases (SFKs), Fig. 6A large arrowhead). All SFKs contain distinct tyrosine residues that, when phosphorylated, are either activating or inhibitory. In Src, these residues are Y416 and Y505 respectively, and the antibodies targeting these sites recognize all SFKs. Probing with phospho-specific antibodies for the active (pY416) and inactive (pY505) forms of SFKs revealed a marked enhancement in tyrosine phosphorylation at the activating site and a decrease in phosphorylation at the inhibitory site (Fig. 6B), indicating a marked increase in the activation state of SFKs in LAT-Y136F CD4^{+} T cells.

This SFK activation could have been due to either an enhanced activation of SFKs normally expressed in T cells (Lck, Fyn, and Yes) or aberrant expression and activation of SFKs not

normally expressed to a significant degree in T lymphocytes (Src, Fgr, Hck, Blk, and Fyn). Immunoprecipitation for the activated form of the SFKs (pY416) followed by blotting for total individual SFKs revealed that Lck, Fyn, and to a lesser extent Yes, but not other SFKs, were hyper-activated in LAT-Y136F CD4$^+$ T lymphocytes (Fig. 6C and data not shown). Furthermore, RasGRP1 deletion did not diminish the high levels of SFK phosphorylation seen in LAT-Y136F CD4$^+$ T lymphocytes suggesting that SFK hyper-activation was upstream of RasGRP1 (Fig. 6D).

Downstream of TCR-MHC engagement, activated SFKs Lck and Fyn normally phosphorylate ITAM domains on the TCRζ and CD3 chains, leading to recruitment and activation of the tyrosine kinase ZAP70 (1). However, LAT-Y136F CD4$^+$ T cells have an activated phenotype [CD44^{hi}CD62L^{lo}CD45RB^{lo}TCRβ^{lo} (14, 16)] and show low surface TCR/CD3 complex expression compatible with activation-induced TCR down-regulation [(14, 16) and Fig. 6E]. Phosphorylation of TCRζ, the major docking site for ZAP70 on the TCR/CD3 complex, was dramatically decreased in LAT-Y136F CD4$^+$ T lymphocytes (Fig. 6E), possibly due to low levels of TCRζ surface expression. Furthermore, the high level of active SFK observed in LAT-Y136F CD4$^+$ T cells was uncoupled from ZAP70, as both phosphorylation of ZAP70 at its active site (Fig. 6B and (17)) and co-immunoprecipitation between Lck and ZAP70 (Fig. 7A) were actually decreased in CD4$^+$ T cells from LAT-Y136F mice compared to WT controls.

Since high levels of SFK activity did not lead to elevated ZAP70 phosphorylation, it seemed unlikely that 'canonical' signaling pathways were contributing to the elevated, RasGRP1-dependent, basal ERK activation observed in LAT-Y136F CD4$^+$ T cells (Fig. 5). We therefore sought to determine whether the elevated SFK signals were shunted to RasGRP1 via normal, alternative signaling pathways. Previous studies have shown that PKCθ can associate with and be activated by the SFK Lck (36–38). We observed enhanced, basal co-immunoprecipitation between Lck and PKCθ in CD4$^+$ T cells isolated from LAT-Y136F mice (Fig. 7A and B). This interaction was specific, as Lck did not co-immunoprecipitate to a detectable level with the closely related PKC family member PKCδ (Fig. 7A).

PKCθ membrane recruitment, which depends upon association of its C1 domain with DAG (39, 40), is enhanced by its association with and activation by Lck (41). We therefore tested whether LAT-Y136F CD4$^+$ T cells showed enhanced PKCθ membrane recruitment (Fig. 7C) and activation (Fig. 7D). PKCθ levels were elevated in crude membrane extracts (P100 fractions) isolated from LAT-Y136F CD4$^+$ T cells compared to WT controls (Fig. 7C), indicating that its DAG-dependent recruitment is elevated in LAT-Y136F CD4$^+$ T cells. Immunoblotting for an activating site (T538) in the activation loop of PKCθ showed enhanced basal phosphorylation of PKCθ in CD4$^+$ T cells isolated from LAT-Y136F mice (Fig. 7D). These data suggest that the elevated SFK activity observed in LAT-Y136F CD4$^+$ T cells could directly signal to PKCθ, leading to elevated PKCθ activation and downstream signaling.

RasGRP1 is a direct target of PKCθ, and activation of RasGRP1 depends upon both its DAG-dependent recruitment to the membrane and on its phosphorylation by PKCθ on T184 (6). RasGRP1 levels were elevated basally in crude membrane extracts (P100 fractions) isolated from LAT-Y136F CD4$^+$ T cells compared to WT controls (Fig. 7C), indicating that its DAG-dependent recruitment is enhanced in LAT-Y136F CD4$^+$ T cells. To assess PKCθ-dependent phosphorylation of RasGRP1, we generated a phospho-specific antibody specific to T184, the site on RasGRP1 phosphorylated by PKCθ (Fig. S1A and B). Similar to PKCθ, phosphorylation of RasGRP1 on T184 was enhanced in LAT-Y136F CD4$^+$ T cells (Fig. 7D). These data (Fig. 6 and 7) are consistent with signals from both activated SFKs and PKCθ emanating to RasGRP1 and ERK in LAT-Y136F CD4$^+$ T cells.

To help determine whether the ERK hyper-activation seen in LAT-Y136F CD4^{+} T lymphocytes was downstream of both the SFKs and PKC, CD4^{+} T lymphocytes isolated from either WT or LAT-Y136F mice were pre-treated with inhibitors of these kinases prior to stimulation with anti-CD3ε + anti-CD4. The SFK inhibitor PP2 (23) efficiently inhibited ERK activation (both basal and stimulated) in both WT and LAT-Y136F CD4^{+} T lymphocytes, indicating that ERK was downstream of SFKs in LAT-Y136F mice (Fig. 8A and B). We next examined whether PKCθ was required for ERK hyper-activation in LAT-Y136F mice. The PKC family of enzymes can be divided into three branches based upon their activation requirements: conventional (DAG- and Ca^{++}-dependent), novel (DAG-dependent but Ca^{++}-independent), and atypical (DAG- and Ca^{++}-independent). To examine PKCθ activation (a novel PKC family member), a combination of inhibitors to either conventional or total (pan-isoform) PKC enzymes was used. The total PKC inhibitor Gö6983 (25) and Rottlerin (which has been reported to inhibit the novel PKCs delta (26) and theta (42)) reduced ERK activation to a much greater extent than the conventional PKC inhibitor Gö6976 (24) (Fig. 8A), supporting the hypothesis that signaling from PKCθ or another novel PKC drives ERK hyper-activation in T cells from LAT-Y136F mice.

PCKθ activation is normally facilitated by PLC-γ1-dependent DAG production. However, while inhibition of PLC-γ1 using U73122 (27, 28) efficiently inhibited ERK activation in CD4^{+} T lymphocytes isolated from WT mice (Fig. 8B), it did not alter the ERK hyper-activation observed in LAT-Y136F mice (Fig. 8A) confirming the PLC-γ1-independent nature of this altered signaling pathway. U73343, an inactive enantiomer of U73122, was used as a control and showed no effect in either WT or LAT-Y136F CD4^{+} T cells. We also tested whether pc-PLC and/or PLD (other phospholipases that contribute to DAG production) substituted for PLC-γ1 in LAT-Y136F mice by using the pc-PLC and PLD inhibitor D609 (29). While D609 partially reduced anti-CD3ε + anti-CD4-stimulated ERK activation in both WT and LAT-Y136F CD4^{+} T cells (Fig. 8A-B), D609 significantly inhibited basal ERK activation in LAT-Y136F CD4^{+} T cells (Fig. 8A). These data suggest that alternative sources of DAG cooperate with Lck/PKCθ signaling to drive RasGRP1 membrane localization (Fig. 7C) and activation (Fig. 7D), leading to basal ERK hyper-activation in T cells from LAT-Y136F mice.

While these data suggest a linear pathway from Lck to RasGRP1 via activation of PKCθ, it still remained formally possible that SFK and PKCθ promote ERK activation independently of RasGRP1. To assess the epistatic nature of SFK, PKCθ, and RasGRP1 signaling to ERK, CD4^{+} T cells from LAT-Y136F were isolated and pre-treated with either SFK (PP2) or PKC [Gö6983 (total PKC) and Rottlerin (PKCθ- and PKCδ-specific)] inhibitors followed by Western blotting for phosphorylated PKCθ and RasGRP1. SFK inhibition significantly inhibited both PCKθ and RasGRP1 phosphorylation, suggesting that SFKs are upstream of both PKCθ and RasGRP1, while PKC inhibition reduced RasGRP1 phosphorylation suggesting that PKCθ is upstream of RasGRP1 in LAT-Y136F CD4^{+} T cells (Fig. 8C). These data suggest a linear signaling sequence emanating from Lck, through PKCθ, to RasGRP1 that drives ERK hyper-activation and disease in LAT-Y136F CD4^{+} mice.

Discussion

Mice encoding a germline mutation in the PLC-γ1 binding site of LAT [LAT-Y136F mice (14, 16)] develop an overwhelming T_H2 CD4^{+} T cell lymphoproliferation that is dependent on the ERK signaling cascade (18). Dissection of signaling pathways upstream of ERK revealed Ras hyper-activation in LAT-Y136F T cells. Ras is activated downstream of the TCR by the combined actions of the RasGEFs RasGRP1, Sos1, and Sos2. RasGRP1 activation normally depends on PLC-γ1-dependent generation of DAG, which acts both directly on RasGRP1 and indirectly by activating PKCθ, which can phosphorylate and

enhance RasGRP1 activity (6). Sos1/2 activation depends both on Grb2-dependent recruitment to LAT and on binding to activated Ras-GTP to enhance Sos catalytic activity (7, 9). We have previously defined a Bam32-dependent pathway in LAT-Y136F mice. LAT-Y136F/Bam32$^{-/-}$ mice show a decrease in ERK activation that correlates with the extent of disease progression. (18). However, in that study it was apparent that the Bam32-dependent pathway was not the exclusive determinant of disease. Based upon a loss of PLC-γ1 activation (16, 17), we had originally hypothesized that the Bam32-independent signaling to ERK seen in LAT-Y136F mice would be Sos1/2-dependent. Therefore we assessed whether Sos1/2 or RasGRP1 deletion could alter the lymphoproliferative phenotype in LAT-Y136F mice.

Surprisingly, RasGRP1 deletion had a more pronounced effect on both ERK1/2 phosphorylation (Fig. 5) and lymphoproliferative disease in LAT-Y136F mice (Fig. 2 and 3) than did Sos1/2 deletion. However, comparison of the effects of Sos1/2 and RasGRP1 in animal models are complicated by both their combined requirements during lymphocyte development (11) and their reported interdependence during TCR-signaling (9). We have previously reported that the combined actions of Sos1 and RasGRP1 are required for pre-TCR-driven proliferation beyond the DN3 checkpoint (11, 22). Furthermore, RasGRP1$^{-/-}$ mice show a significant block in positive selection (19). Therefore, developmental effects caused by these knockout models, in conjunction with the developmental effects caused by the LAT-Y136F mutation (16, 43), can complicate interpretation of alterations in the disease state of the animals. Using Sos1(T)$^{-/-}$ and Sos1/2 DKO mice (which have identical effects on thymocyte development when crossed to a LAT-Y136F background (Fig. 4)) we found that indeed Sos1/2 DKO altered LAT-Y136F lymphoproliferative disease independent of altering thymocyte development.

It remained unclear, however, whether the effect of Sos1/2 deletion was a direct consequence of LAT/Grb2-mediated Sos1/2 activation or to the presence of a RasGRP1/Ras/Sos/Ras positive feedback loop (8, 9). When assessing the effects of Sos1/2 and RasGRP1 deletion, each RasGEF KO independently delayed disease progression in LAT-Y136F mice (Table SI). Comparison between these two groups showed less CD4^{+} lymphocyte accumulation in LAT-Y136F/RasGRP1$^{-/-}$ than in LAT-Y136F/Sos1/2 DKO mice (Fig. 3A). These data are compatible with RasGRP1 being dominant to Sos1/2, with the contribution of Sos1/2 limited to a potential RasGRP1/Ras/Sos positive feedback loop. However, effects on disease progression between these two groups were not statistically different (Fig. 2A, P=0.07). Since these two groups may have similar rates of disease progression (Fig. 2A, Table SI) but differences in accumulated disease at a given time (7 and 14 weeks, Fig. 3A), we cannot rule out the possibility that some of differences observed between RasGRP1 and Sos1/2 deletion are due to developmental effects due to RasGRP1 deficiency.

We observed a complete loss of lymphoproliferative disease in LAT- LAT-Y136F/RasGRP1$^{-/-}$/Sos1/2 DKO mice, suggesting that Sos1/2 cannot be completely downstream of RasGRP1, otherwise the LAT-Y136F/RasGRP1$^{-/-}$ and LAT-Y136F/Sos1/2 DKO/RasGRP1$^{-/-}$ phenotypes would be identical. However, the rate of disease progression in LAT-Y136F/Sos1/2 DKO/RasGRP1$^{-/-}$ mice was different than LAT-Y136F/Sos1/2 DKO mice, but not LAT-Y136F/RasGRP1$^{-/-}$ mice. These data suggest that RasGRP1 is the dominant RasGEF driving the disease phenotype. A complete understanding of the interplay between Sos1/2 and RasGRP1, and how the RasGEF-dependent pathways are tied into Bam32-dependent signaling in LAT-Y136F mice will require combined RasGRP1/Bam32 and/or Sos1/2/Bam32 deletion on a LAT-Y136F background.

We (16, 18, 43) and others (14, 17, 44) simultaneously generated and described LAT-Y136F mice. However, while the overall phenotypes of these mice are strikingly similar, dissection of the molecular mechanisms that drive disease initiation and progression have yielded divergent conclusions. When examining TCR (α-CD3- + α-CD4-induced) signaling in LAT-Y136F CD4$^+$ T cells, both laboratories have reported defective or absent LAT phosphorylation, PLC-γ1 phosphorylation, and Ca^{++} flux (16, 17) whereas examination of ERK activation has yielded differing results. We observe ERK hyper-activation (18) whereas the Malissen group does not see ERK activation (17) in LAT-Y136F CD4$^+$ T cells. While we do not understand the difference observed between the two laboratories, one possibility relates to our finding that the timing of the signaling experiments after dissection is critical. Our signaling experiments have revealed that while freshly isolated LAT-Y136F CD4$^+$ T lymphocytes show high basal activation of SFK/Ras/ERK signaling, significant resting of cells post-isolation can either reduce this basal ERK signaling (after 5 hours) [(18) and data not shown] or eliminate differences in ERK activation from WT mice (after overnight culture) (16).

By examining upstream signaling in freshly isolated cells, we found basal and TCR-stimulated SFK hyper-activation in LAT-Y136F CD4$^+$ T cells (Fig. 6). While we still do not fully understand the origin of SFK hyper-activation in LAT-Y136F mice, we hypothesize that the unique signaling environment caused by the marked TCR-CD3 complex down-regulation seen in LAT-Y136F CD4$^+$ T cells [Fig. 6E and (14, 16)] underlies many of the signaling anomalies. In LAT-Y136F CD4$^+$ T cells, there is very low/undetectable TCRζ phosphorylation (Fig. 6E), an adaptation likely responsible for the decrease in ZAP70 docking and activation. This reduced TCRζ phosphorylation may account for the inefficiency in Lck-ZAP70 interaction (Fig. 7A) and ZAP70 phosphorylation (Fig. 6B) seen in LAT-Y136F CD4$^+$ T cells.

The loss of canonical ZAP70 signaling could potentially modify activity of one of several regulatory axes controlling SFK activity, for example Csk-CD45 signaling (45, 46), Shp-1/ERK signaling (47), or signaling through the E3 ubiquitin ligase Cbl (48). Alternatively, feedback regulation of ZAP70 by the adaptor and LAT binding partner SLP-76 has been reported, with both ZAP70 phosphorylation and clustering being inhibited in SLP-76 deficient Jurkat cells (49, 50). Furthermore, it has been suggested that LAT itself is a negative regulator of T cell signaling by an unknown mechanism (51). However, whether SLP-76 and/or LAT truly exhibit a level of feedback regulation on SFK remains to be seen.

We therefore sought to determine whether the elevated SFK signals were shunted to RasGRP1 via alternative signaling pathways and identified an SFK/PKCθ/RasGRP1 signaling pathway that became dominant in the altered signaling environment created by the LAT-Y136F mutation. There exists significant precedence for the existence of SFK-dependent, ZAP70-and LAT-independent, signaling in T cells. First, studies using ZAP70-deficient Jurkat cells have shown SFK and PKC-dependent, ZAP70-independent ERK activation (52). Secondly, previous studies have shown that, in addition to DAG-dependent recruitment (39, 40), PKCθ activation requires its localization to lipid rafts and is Lck-dependent, but ZAP70-independent (36). Furthermore, Lck has been shown to co-precipitate with and directly phosphorylate PKCθ (37), and Lck-dependent phosphorylation of PKCθ enhances the membrane targeting and activation of PKCθ (41).

In LAT-Y136F CD4$^+$ T cells, we find enhanced basal association of Lck with PKCθ (Fig. 7A and B), which both enhanced the DAG-mediated membrane recruitment (Fig. 7C) and led to the activation of PKCθ (Fig. 7D). Furthermore, inhibition of SFK signaling reduced the activation of PKCθ (Fig. 8C). Once activated, PKCθ can directly phosphorylate and help activate RasGRP1. We observe elevated basal RasGRP1 phosphorylation on T184 (Fig. 7D)

that was decreased by total, but not typical PKC inhibition (Fig. 8C). These data suggest that the elevated PKCθ phosphorylation (Fig. 7D), downstream of SFK hyper-activation (Fig. 6B), activates RasGRP1/ERK signaling.

Studies using mutated, pathologic cells have led to the understanding of many fundamental signaling proteins including Src (53–55) and Ras (56, 57), or novel signaling connections now recognized as important to normal cellular function (58). In T cells, much of our understanding of the molecular details of downstream TCR signaling comes from studying T cell leukemia cells and mutant animal models. Relevant to this study is that in addition to LAT-Y136F mutant mice, multiple animal models carrying mutations in TCR- and/or IL-2-dependent signaling [including IL-2$^{-/-}$ (59), STAT5a/5b DKO (60), STIM1/2 DKO (61), NFATc2/c3 DKO (62), Vav1$^{-/-}$Cbl-b$^{-/-}$ (63), and CD45-E613R mice (64)] show a lymphoproliferative phenotype. Maintenance of proper signaling through these proteins and their downstream signaling targets likely represents an important physiological barrier to the development of lymphoproliferative disease.

When trying to understand the molecular mechanisms driving lymphoproliferation in LAT-Y136F mice, we noticed an unexpected ERK hyper-activation, and have sought to explain both the origin and significance of ERK activation in these mice. Through the course of these studies, we have tested various mouse models known to signal to the ERK pathway, first describing a LAT-independent, Bam32-dependent pathway that accounts for some, but not all, of the ERK hyper-activation in LAT-Y136F mice (18). Based upon these studies, we have recently defined a novel PLC-γ1/Bam32/PAK1 signaling pathway to ERK, which is independent of PLC-γ1 catalytic activity and functions under normal physiologic conditions (65). Here, we describe how known, albeit less well understood, signaling connections can be re-wired to produce pathologic RasGRP1-dependent Ras/ERK activation. These studies show that a tremendous amount of plasticity exists in TCR-dependent signaling, and that perturbation of 'canonical' signaling pathways, while predicted to blunt signaling, may have unknown pathologic consequences. Understanding how the signaling environment is changed in these settings enhances our understanding of normal, alternative signaling pathways. Furthermore, these studies inform future targeted therapeutic choices by revealing both those signaling molecules that may represent good candidate targets and which perturbations might have unforeseen adverse consequences.

Supplementary Material

Refer to Web version on PubMed Central for supplementary material.

Acknowledgments

References

1. Smith-Garvin JE, Koretzky GA, Jordan MS. T cell activation. Annu Rev Immunol. 2009; 27:591–619. [PubMed: 19132916]

2. Zhu M, Janssen E, Zhang W. Minimal requirement of tyrosine residues of linker for activation of T cells in TCR signaling and thymocyte development. J Immunol. 2003; 170:325–333. [PubMed: 12496416]

3. Balagopalan L, Coussens NP, Sherman E, Samelson LE, Sommers CL. The LAT story: a tale of cooperativity, coordination, and choreography. Cold Spring Harb Perspect Biol. 2010; 2:a005512. [PubMed: 20610546]

4. Zhang W, Sloan-Lancaster J, Kitchen J, Trible RP, Samelson LE. LAT: the ZAP-70 tyrosine kinase substrate that links T cell receptor to cellular activation. Cell. 1998; 92:83–92. [PubMed: 9489702]

5. Zhang W, Trible RP, Zhu M, Liu SK, McGlade CJ, Samelson LE. Association of Grb2, Gads, and phospholipase C-gamma 1 with phosphorylated LAT tyrosine residues. Effect of LAT tyrosine mutations on T cell angigen receptor-mediated signaling. J Biol Chem. 2000; 275:23355–23361. [PubMed: 10811803]

6. Roose JP, Mollenauer M, Gupta VA, Stone J, Weiss A. A diacylglycerol-protein kinase C-RasGRP1 pathway directs Ras activation upon antigen receptor stimulation of T cells. Mol Cell Biol. 2005; 25:4426–4441. [PubMed: 15899849]

7. Margarit SM, Sondermann H, Hall BE, Nagar B, Hoelz A, Pirruccello M, Bar-Sagi D, Kuriyan J. Structural evidence for feedback activation by Ras.GTP of the Ras-specific nucleotide exchange factor SOS. Cell. 2003; 112:685–695. [PubMed: 12628188]

8. Das J, Ho M, Zikherman J, Govern C, Yang M, Weiss A, Chakraborty AK, Roose JP. Digital signaling and hysteresis characterize ras activation in lymphoid cells. Cell. 2009; 136:337–351. [PubMed: 19167334]

9. Roose JP, Mollenauer M, Ho M, Kurosaki T, Weiss A. Unusual interplay of two types of Ras activators, RasGRP and SOS, establishes sensitive and robust Ras activation in lymphocytes. Mol Cell Biol. 2007; 27:2732–2745. [PubMed: 17283063]

10. Genot E, Cantrell DA. Ras regulation and function in lymphocytes. Curr Opin Immunol. 2000; 12:289–294. [PubMed: 10781411]

11. Kortum RL, Sommers CL, Pinski JM, Alexander CP, Merrill RK, Li W, Love PE, Samelson LE. Deconstructing Ras signaling in the thymus. Mol Cell Biol. 2012; 32:2748–2759. [PubMed: 22586275]

12. Zhang W, Sommers CL, Burshtyn DN, Stebbins CC, DeJarnette JB, Trible RP, Grinberg A, Tsay HC, Jacobs HM, Kessler CM, Long EO, Love PE, Samelson LE. Essential role of LAT in T cell development. Immunity. 1999; 10:323–332. [PubMed: 10204488]

13. Sommers CL, Menon RK, Grinberg A, Zhang W, Samelson LE, Love PE. Knock-in mutation of the distal four tyrosines of linker for activation of T cells blocks murine T cell development. J Exp Med. 2001; 194:135–142. [PubMed: 11457888]

14. Aguado E, Richelme S, Nunez-Cruz S, Miazek A, Mura AM, Richelme M, Guo XJ, Sainty D, He HT, Malissen B, Malissen M. Induction of T helper type 2 immunity by a point mutation in the LAT adaptor. Science. 2002; 296:2036–2040. [PubMed: 12065839]

15. Nunez-Cruz S, Aguado E, Richelme S, Chetaille B, Mura AM, Richelme M, Pouyet L, Jouvin-Marche E, Xerri L, Malissen B, Malissen M. LAT regulates gammadelta T cell homeostasis and differentiation. Nat Immunol. 2003; 4:999–1008. [PubMed: 12970761]

16. Sommers CL, Park CS, Lee J, Feng C, Fuller CL, Grinberg A, Hildebrand JA, Lacana E, Menon RK, Shores EW, Samelson LE, Love PE. A LAT mutation that inhibits T cell development yet induces lymphoproliferation. Science. 2002; 296:2040–2043. [PubMed: 12065840]

17. Mingueneau M, Roncagalli R, Gregoire C, Kissenpfennig A, Miazek A, Archambaud C, Wang Y, Perrin P, Bertosio E, Sansoni A, Richelme S, Locksley RM, Aguado E, Malissen M, Malissen B. Loss of the LAT adaptor converts antigen-responsive T cells into pathogenic effectors that function independently of the T cell receptor. Immunity. 2009; 31:197–208. [PubMed: 19682930]

18. Miyaji M, Kortum RL, Surana R, Li W, Woolard KD, Simpson RM, Samelson LE, Sommers CL. Genetic evidence for the role of Erk activation in a lymphoproliferative disease of mice. Proc Natl Acad Sci U S A. 2009; 106:14502–14507. [PubMed: 19667175]

19. Dower NA, Stang SL, Bottorff DA, Ebinu JO, Dickie P, Ostergaard HL, Stone JC. RasGRP is essential for mouse thymocyte differentiation and TCR signaling. Nat Immunol. 2000; 1:317–321. [PubMed: 11017103]

20. Esteban LM, Fernandez-Medarde A, Lopez E, Yienger K, Guerrero C, Ward JM, Tessarollo L, Santos E. Ras-guanine nucleotide exchange factor sos2 is dispensable for mouse growth and development. Mol Cell Biol. 2000; 20:6410–6413. [PubMed: 10938118]

21. Lee PP, Fitzpatrick DR, Beard C, Jessup HK, Lehar S, Makar KW, Perez-Melgosa M, Sweetser MT, Schlissel MS, Nguyen S, Cherry SR, Tsai JH, Tucker SM, Weaver WM, Kelso A, Jaenisch R, Wilson CB. A critical role for Dnmt1 and DNA methylation in T cell development, function, and survival. Immunity. 2001; 15:763–774. [PubMed: 11728338]

22. Kortum RL, Sommers CL, Alexander CP, Pinski JM, Li W, Grinberg A, Lee J, Love PE, Samelson LE. Targeted Sos1 deletion reveals its critical role in early T-cell development. Proc Natl Acad Sci U S A. 2011; 108:12407–12412. [PubMed: 21746917]

23. Hanke JH, Gardner JP, Dow RL, Changelian PS, Brissette WH, Weringer EJ, Pollok BA, Connelly PA. Discovery of a novel, potent, and Src family-selective tyrosine kinase inhibitor. Study of Lck- and FynT-dependent T cell activation. J Biol Chem. 1996; 271:695–701. [PubMed: 8557675]

24. Martiny-Baron G, Kazanietz MG, Mischak H, Blumberg PM, Kochs G, Hug H, Marme D, Schachtele C. Selective inhibition of protein kinase C isozymes by the indolocarbazole Go 6976. J Biol Chem. 1993; 268:9194–9197. [PubMed: 8486620]

25. Toullec D, Pianetti P, Coste H, Bellevergue P, Grand-Perret T, Ajakane M, Baudet V, Boissin P, Boursier E, Loriolle F, et al. The bisindolylmaleimide GF 109203X is a potent and selective inhibitor of protein kinase C. J Biol Chem. 1991; 266:15771–15781. [PubMed: 1874734]

26. Gschwendt M, Muller HJ, Kielbassa K, Zang R, Kittstein W, Rincke G, Marks F. Rottlerin, a novel protein kinase inhibitor. Biochem Biophys Res Commun. 1994; 199:93–98. [PubMed: 8123051]

27. Ebinu JO, Stang SL, Teixeira C, Bottorff DA, Hooton J, Blumberg PM, Barry M, Bleakley RC, Ostergaard HL, Stone JC. RasGRP links T-cell receptor signaling to Ras. Blood. 2000; 95:3199–3203. [PubMed: 10807788]

28. Bleasdale JE, Bundy GL, Bunting S, Fitzpatrick FA, Huff RM, Sun FF, Pike JE. Inhibition of phospholipase C dependent processes by U-73, 122. Adv Prostaglandin Thromboxane Leukot Res. 1989; 19:590–593. [PubMed: 2526542]

29. Kim JG, Shin I, Lee KS, Han JS. D609-sensitive tyrosine phosphorylation is involved in Fas-mediated phospholipase D activation. Exp Mol Med. 2001; 33:303–309. [PubMed: 11795496]

30. Favata MF, Horiuchi KY, Manos EJ, Daulerio AJ, Stradley DA, Feeser WS, Van Dyk DE, Pitts WJ, Earl RA, Hobbs F, Copeland RA, Magolda RL, Scherle PA, Trzaskos JM. Identification of a novel inhibitor of mitogen-activated protein kinase kinase. J Biol Chem. 1998; 273:18623–18632. [PubMed: 9660836]

31. Castro AF, Rebhun JF, Quilliam LA. Measuring Ras-family GTP levels in vivo--running hot and cold. Methods. 2005; 37:190–196. [PubMed: 16289967]

32. Wange RL, Guitian R, Isakov N, Watts JD, Aebersold R, Samelson LE. Activating and inhibitory mutations in adjacent tyrosines in the kinase domain of ZAP-70. J Biol Chem. 1995; 270:18730–18733. [PubMed: 7642520]

33. Orloff DG, Frank SJ, Robey FA, Weissman AM, Klausner RD. Biochemical characterization of the eta chain of the T-cell receptor. A unique subunit related to zeta. J Biol Chem. 1989; 264:14812–14817. [PubMed: 2768241]

34. Roy S, Lane A, Yan J, McPherson R, Hancock JF. Activity of plasma membrane-recruited Raf-1 is regulated by Ras via the Raf zinc finger. J Biol Chem. 1997; 272:20139–20145. [PubMed: 9242688]

35. Mor A, Philips MR. Compartmentalized Ras/MAPK signaling. Annu Rev Immunol. 2006; 24:771–800. [PubMed: 16551266]

36. Bi K, Tanaka Y, Coudronniere N, Sugie K, Hong S, van Stipdonk MJ, Altman A. Antigen-induced translocation of PKC-theta to membrane rafts is required for T cell activation. Nat Immunol. 2001; 2:556–563. [PubMed: 11376344]

37. Liu Y, Witte S, Liu YC, Doyle M, Elly C, Altman A. Regulation of protein kinase Ctheta function during T cell activation by Lck-mediated tyrosine phosphorylation. J Biol Chem. 2000; 275:3603–3609. [PubMed: 10652356]

38. Kong KF, Yokosuka T, Canonigo-Balancio AJ, Isakov N, Saito T, Altman A. A motif in the V3 domain of the kinase PKC-theta determines its localization in the immunological synapse and functions in T cells via association with CD28. Nat Immunol. 2011; 12:1105–1112. [PubMed: 21964608]

39. Carrasco S, Merida I. Diacylglycerol-dependent binding recruits PKCtheta and RasGRP1 C1 domains to specific subcellular localizations in living T lymphocytes. Mol Biol Cell. 2004; 15:2932–2942. [PubMed: 15064353]

40. Diaz-Flores E, Siliceo M, Martinez AC, Merida I. Membrane translocation of protein kinase Ctheta during T lymphocyte activation requires phospholipase C-gamma-generated diacylglycerol. J Biol Chem. 2003; 278:29208–29215. [PubMed: 12738795]

41. Melowic HR, Stahelin RV, Blatner NR, Tian W, Hayashi K, Altman A, Cho W. Mechanism of diacylglycerol-induced membrane targeting and activation of protein kinase Ctheta. J Biol Chem. 2007; 282:21467–21476. [PubMed: 17548359]

42. Springael C, Thomas S, Rahmouni S, Vandamme A, Goldman M, Willems F, Vosters O. Rottlerin inhibits human T cell responses. Biochem Pharmacol. 2007; 73:515–525. [PubMed: 17141738]

43. Sommers CL, Lee J, Steiner KL, Gurson JM, Depersis CL, El-Khoury D, Fuller CL, Shores EW, Love PE, Samelson LE. Mutation of the phospholipase C-gamma1-binding site of LAT affects both positive and negative thymocyte selection. J Exp Med. 2005; 201:1125–1134. [PubMed: 15795236]

44. Genton C, Wang Y, Izui S, Malissen B, Delsol G, Fournie GJ, Malissen M, Acha-Orbea H. The Th2 lymphoproliferation developing in LatY136F mutant mice triggers polyclonal B cell activation and systemic autoimmunity. J Immunol. 2006; 177:2285–2293. [PubMed: 16887989]

45. Schoenborn JR, Tan YX, Zhang C, Shokat KM, Weiss A. Feedback circuits monitor and adjust basal Lck-dependent events in T cell receptor signaling. Sci Signal. 2011; 4:ra59. [PubMed: 21917715]

46. Zikherman J, Jenne C, Watson S, Doan K, Raschke W, Goodnow CC, Weiss A. CD45-Csk phosphatase-kinase titration uncouples basal and inducible T cell receptor signaling during thymic development. Immunity. 2010; 32:342–354. [PubMed: 20346773]

47. Stefanova I, Hemmer B, Vergelli M, Martin R, Biddison WE, Germain RN. TCR ligand discrimination is enforced by competing ERK positive and SHP-1 negative feedback pathways. Nat Immunol. 2003; 4:248–254. [PubMed: 12577055]

48. Rao N, Miyake S, Reddi AL, Douillard P, Ghosh AK, Dodge IL, Zhou P, Fernandes ND, Band H. Negative regulation of Lck by Cbl ubiquitin ligase. Proc Natl Acad Sci U S A. 2002; 99:3794–3799. [PubMed: 11904433]

49. Liu H, Purbhoo MA, Davis DM, Rudd CE. SH2 domain containing leukocyte phosphoprotein of 76-kDa (SLP-76) feedback regulation of ZAP-70 microclustering. Proc Natl Acad Sci U S A. 2010; 107:10166–10171. [PubMed: 20534575]

50. Brockmeyer C, Paster W, Pepper D, Tan CP, Trudgian DC, McGowan S, Fu G, Gascoigne NR, Acuto O, Salek M. T cell receptor (TCR)-induced tyrosine phosphorylation dynamics identifies THEMIS as a new TCR signalosome component. J Biol Chem. 2011; 286:7535–7547. [PubMed: 21189249]

51. Malbec O, Malissen M, Isnardi I, Lesourne R, Mura AM, Fridman WH, Malissen B, Daeron M. Linker for activation of T cells integrates positive and negative signaling in mast cells. J Immunol. 2004; 173:5086–5094. [PubMed: 15470052]

52. Shan X, Balakir R, Criado G, Wood JS, Seminario MC, Madrenas J, Wange RL. Zap-70-independent Ca(2+) mobilization and Erk activation in Jurkat T cells in response to T-cell antigen receptor ligation. Mol Cell Biol. 2001; 21:7137–7149. [PubMed: 11585897]

53. Brugge JS, Erikson RL. Identification of a transformation-specific antigen induced by an avian sarcoma virus. Nature. 1977; 269:346–348. [PubMed: 198667]

54. Collett MS, Brugge JS, Erikson RL. Characterization of a normal avian cell protein related to the avian sarcoma virus transforming gene product. Cell. 1978; 15:1363–1369. [PubMed: 83198]

55. Levinson AD, Oppermann H, Levintow L, Varmus HE, Bishop JM. Evidence that the transforming gene of avian sarcoma virus encodes a protein kinase associated with a phosphoprotein. Cell. 1978; 15:561–572. [PubMed: 214242]

56. Langbeheim H, Shih TY, Scolnick EM. Identification of a normal vertebrate cell protein related to the p21 src of Harvey murine sarcoma virus. Virology. 1980; 106:292–300. [PubMed: 6254252]

57. Shih TY, Papageorge AG, Stokes PE, Weeks MO, Scolnick EM. Guanine nucleotide-binding and autophosphorylating activities associated with the p21src protein of Harvey murine sarcoma virus. Nature. 1980; 287:686–691. [PubMed: 6253810]

58. Zimmermann S, Moelling K. Phosphorylation and regulation of Raf by Akt (protein kinase B). Science. 1999; 286:1741–1744. [PubMed: 10576742]

59. Gaffen SL, Liu KD. Overview of interleukin-2 function, production and clinical applications. Cytokine. 2004; 28:109–123. [PubMed: 15473953]

60. Snow JW, Abraham N, Ma MC, Herndier BG, Pastuszak AW, Goldsmith MA. Loss of tolerance and autoimmunity affecting multiple organs in STAT5A/5B-deficient mice. J Immunol. 2003; 171:5042–5050. [PubMed: 14607901]

61. Oh-Hora M, Yamashita M, Hogan PG, Sharma S, Lamperti E, Chung W, Prakriya M, Feske S, Rao A. Dual functions for the endoplasmic reticulum calcium sensors STIM1 and STIM2 in T cell activation and tolerance. Nat Immunol. 2008; 9:432–443. [PubMed: 18327260]

62. Ranger AM, Oukka M, Rengarajan J, Glimcher LH. Inhibitory function of two NFAT family members in lymphoid homeostasis and Th2 development. Immunity. 1998; 9:627–635. [PubMed: 9846484]

63. Krawczyk C, Bachmaier K, Sasaki T, Jones RG, Snapper SB, Bouchard D, Kozieradzki I, Ohashi PS, Alt FW, Penninger JM. Cbl-b is a negative regulator of receptor clustering and raft aggregation in T cells. Immunity. 2000; 13:463–473. [PubMed: 11070165]

64. Majeti R, Xu Z, Parslow TG, Olson JL, Daikh DI, Killeen N, Weiss A. An inactivating point mutation in the inhibitory wedge of CD45 causes lymphoproliferation and autoimmunity. Cell. 2000; 103:1059–1070. [PubMed: 11163182]

65. Rouquette-Jazdanian AK, Sommers CL, Kortum RL, Morrison DK, Samelson LE. LAT-Independent Erk activation via Bam32-PLC-g1-PAK1 Complexes: GTPase-Independent PAK1 activation. Mol Cell. 2012 in press.
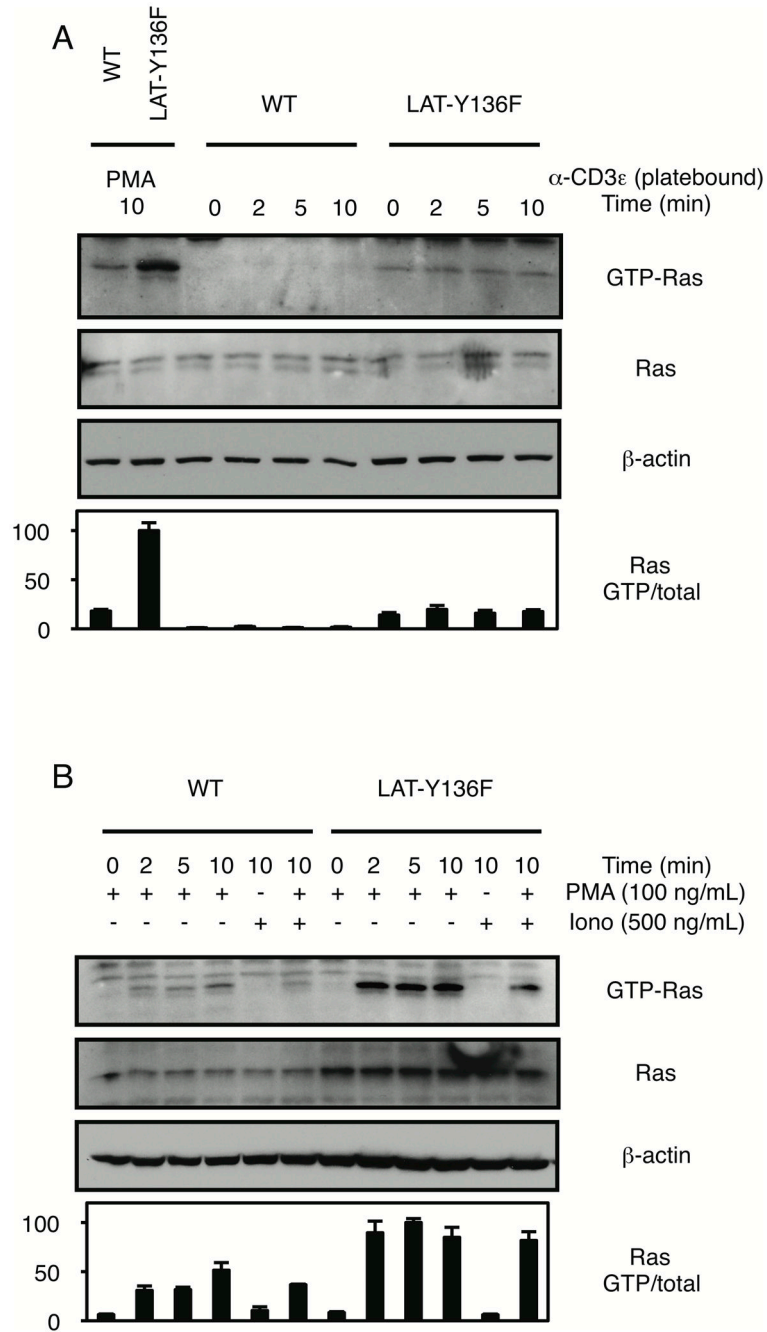
FIGURE 1. CD4^{+} T cells isolated from LAT-Y136F mice show elevated Ras activation
(A–B) Western blotting(above, quantified below) for activated Ras from a GST-RBD pulldown (top) or for total Ras or β-actin in whole cell lysates (WCL) from purified CD4^{+} LN cells from WT versus LAT-Y136F mice stimulated with (A) either 100 ng/mL PMA for ten minutes or 5 μg/mL platebound anti-CD3ε antibody for the indicated times or (B) 100 ng/mL PMA +/− 500 ng/mL Ionomycin for the indicated times. Data are representative of two independent experiments.
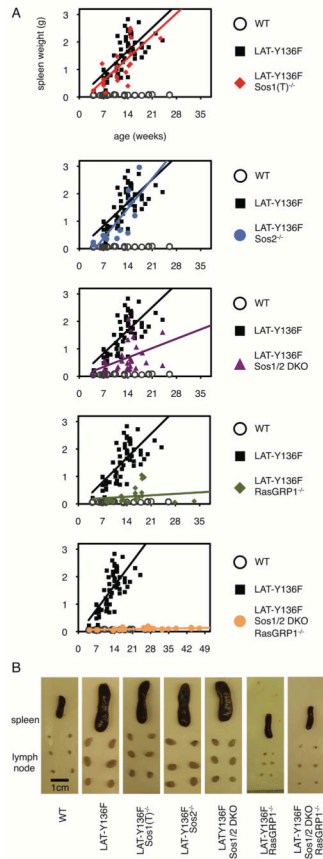
FIGURE 2. RasGRP1, and not Sos1/2, is the major RasGEF responsible for splenomegaly in LAT-Y136F mice

(A) Quantification of spleen weight versus time from WT mice, LAT-Y136F mice, LAT-Y136F mice deleted for Sos1 and/or Sos2, or LAT-Y136F mice deleted for RasGRP1 and/or Sos1/2. Each symbol represents one mouse. Data were accumulated over time from several experiments, and the same accumulated data from WT and LAT-Y136F mice are shown in each graph as controls to compare the LAT-Y136F/RasGEF crosses. LAT-Y136F/Sos1/2 DKO, LAT-Y136F/RasGRP1$^{-/-}$, and LAT-Y136F/Sos1/2 DKO/RasGRP1$^{-/-}$ mice showed significant differences in the slope of the regression line ($p<0.05$) from LAT-Y136F, LAT-Y136F/Sos1$^{-/-}$, or LAT-Y136F/Sos2$^{-/-}$ mice indicating a significant slowing of disease progression upon deletion of Sos1/2 and/or RasGRP1. In contrast, a similar rate in disease progression was noted when comparing LAT-Y136F/Sos1/2 DKO to LAT-Y136F/RasGRP1$^{-/-}$ mice. A complete statistical analysis of the data is given in Table SI.

(B) Photographs of spleen (above) and isolated axillary, brachial, and inguinal lymph nodes (below) from 7-week-old mice indicated in A.
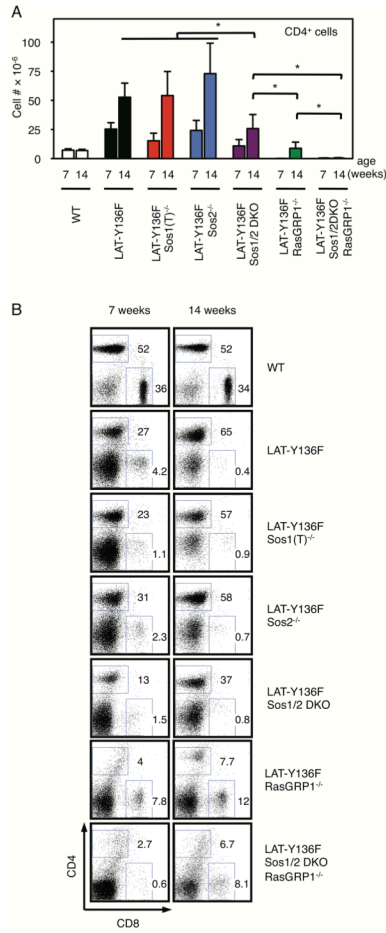
FIGURE 3. RasGRP1, and not Sos1/2, is the major RasGEF responsible for lymphoproliferation in LAT-Y136F mice

(**A**) Quantification of CD4^{+} LN T cell numbers from pooled axillary, brachial, and inguinal lymph nodes stained with anti-CD4 and anti-CD8 from 7 or 14-week-old mice indicated in Fig. 2. n 4 for each group. Data are represented as mean+/− SD. * p<0.05.

(**B**) Flow cytometry dot plots of pooled axillary, brachial, and inguinal lymph nodes stained with anti-CD4 and anti-CD8 from mice indicated in A.
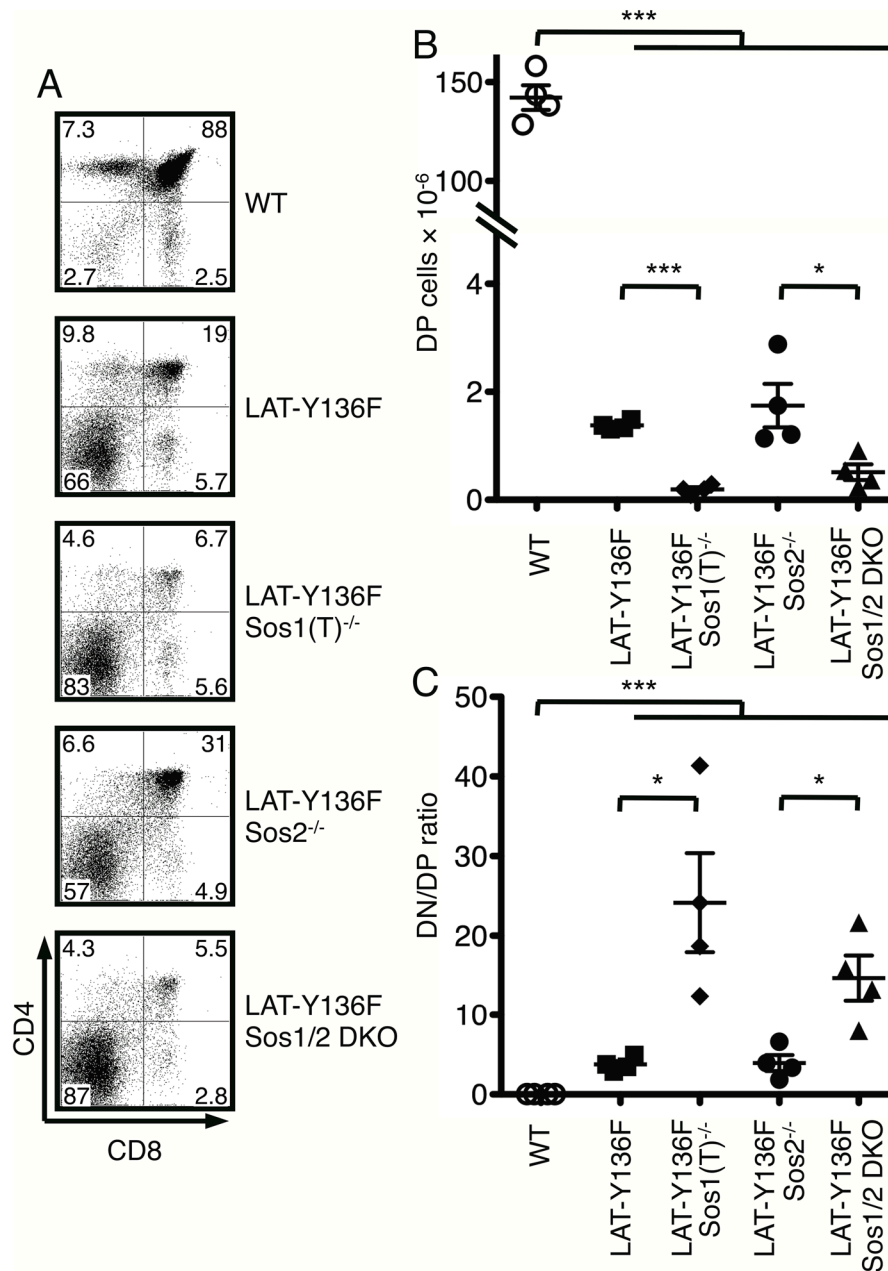
FIGURE 4. Sos1-dependent pre-TCR developmental block does not correlate with delayed disease in LAT-Y136F mice

(**A**) Flow cytometry dot plots of thymocytes stained with anti-CD4 and anti-CD8 from 4-week-old WT mice, LAT-Y136F mice, or LAT-Y136F mice deleted for Sos1 and/or Sos2. n=4 for each group.

(**B**) Total numbers of DP thymocytes isolated from 4-week-old mice from (A) (n=4 for each). Each symbol denotes an individual mouse and the bar denotes the average for the group. * p<0.05, ***p<0.001.<n=br>(**C**) The DN/DP ratio from (A). * p<0.05, ***p<0.001.
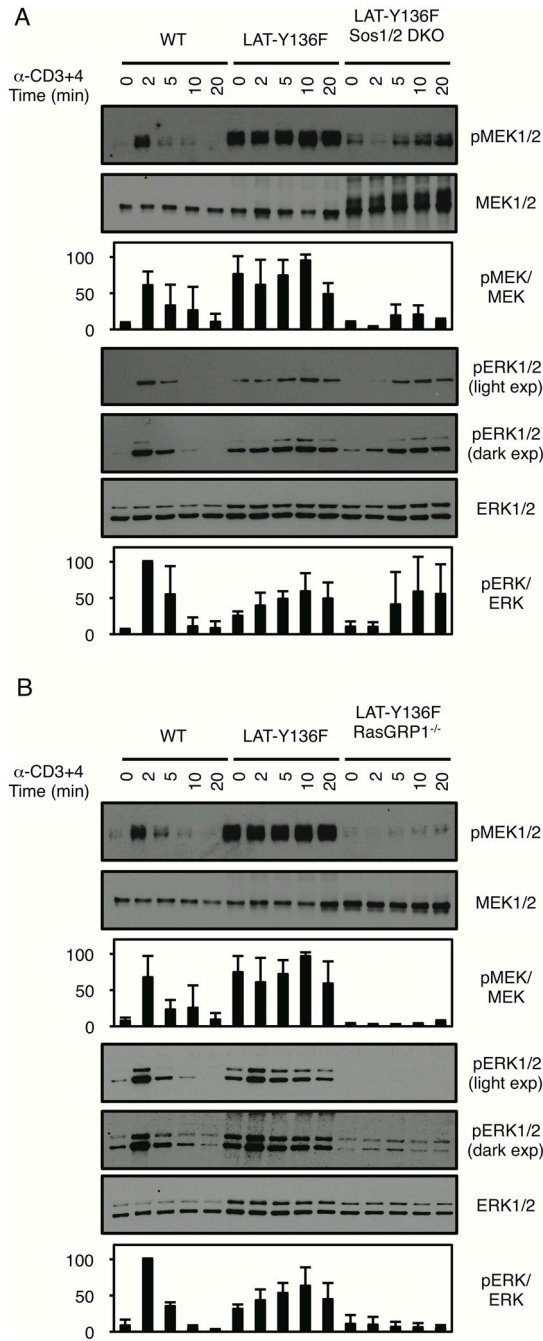
FIGURE 5. RasGRP1 is the major RasGEF responsible for ERK activation in T cells from LAT-Y136F mice

(A–B) Western blotting (above, quantified below) for phospho-MEK, total MEK, phospho-ERK, or total ERK in WCL from purified CD4^{+} LN cells from WT, LAT-Y136F, or LAT-Y136F mice crossed to Sos1/2 DKO mice (A) or RasGRP1^{−/−} mice (B) stimulated with 10 µg/mL soluble anti-CD3ε + anti-CD4 antibodies. All stimulations were for the indicated times in minutes. Total MEK blots were loaded in parallel, and run at the same time as pMEK blots. Data are representative of three independent experiments.
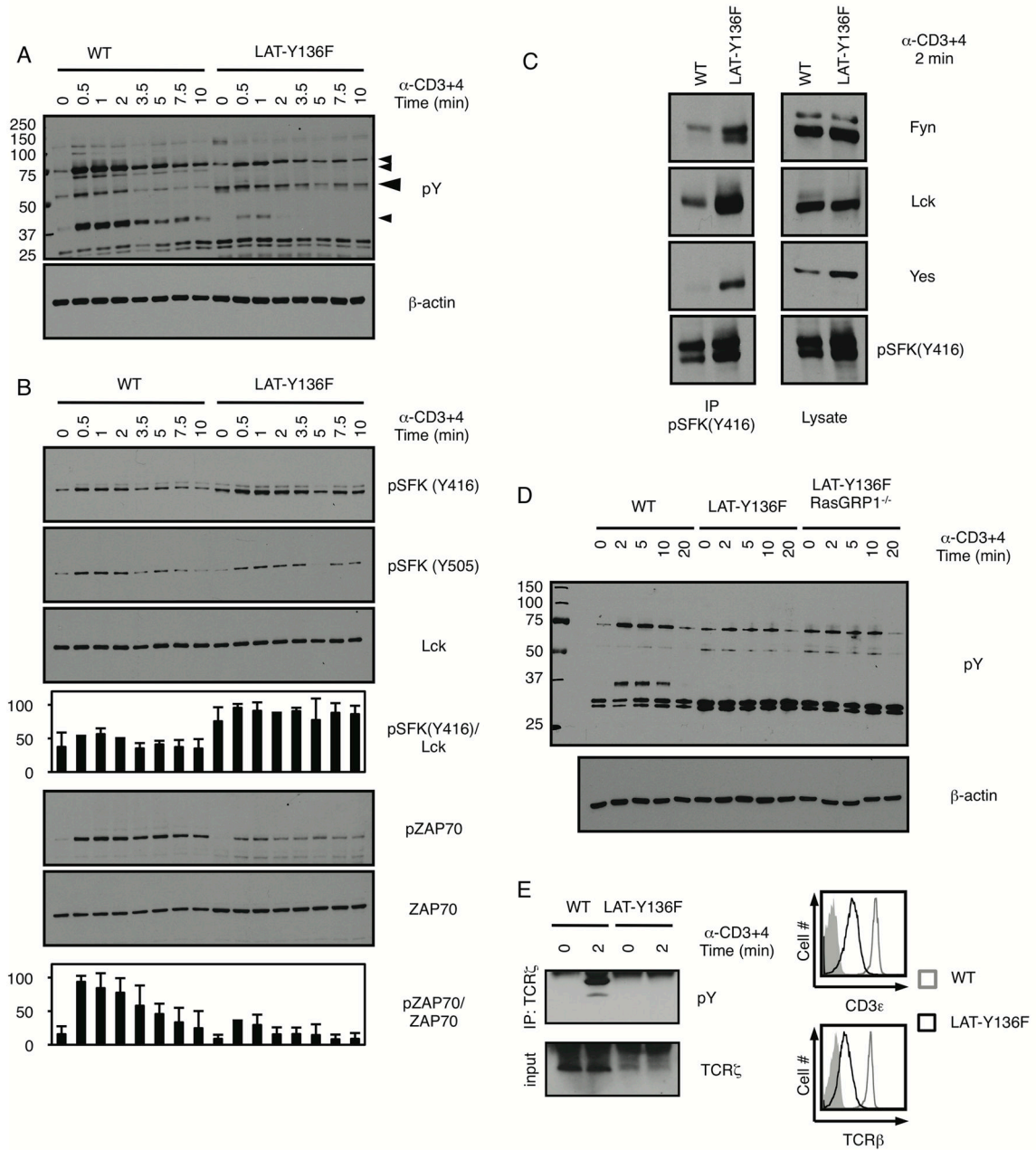
FIGURE 6. Altered activation of upstream kinases in T cells from LAT-Y136F mice
(A–B) Western blotting for phospho-tyrosine (4G10) and β-actin (A), or active phospho-pan Src (Y416), inactive phospho-pan Src (Y505), total Lck, phospho-ZAP70, and total ZAP70 (above, quantified below) (B) in WCL from purified CD4^{+} LN cells from WT and LAT-Y136F mice stimulated with 10 μg/mL soluble anti-CD3ε + anti-CD4 antibodies for the indicated times in minutes. On the phospho-tyrosine blot, small arrowheads represent putative SLP-76, ZAP70, and LAT bands and the large arrowhead a putative SFK doublet as outlined in the text. Data are representative of two independent experiments.
(C) Western blotting for Lck, Fyn, Yes, and phospho-pan Src (Y416) in anti-phospho-pan Src (Y416) immunoprecipitates (left) or WCL (right) from purified CD4^{+} LN cells from WT and LAT-Y136F mice stimulated with 10 μg/mL soluble anti-CD3ε + anti-CD4 antibodies for 2 minutes. Data are representative of two independent experiments.

(D) Western blotting for phospho-tyrosine (4G10) and β-actin in WCL from purified CD4^{+} LN cells from WT, LAT-Y136F, and LAT-Y136F/RasGRP1^{−/−} mice stimulated with 10 μg/mL soluble anti-CD3ε + anti-CD4 antibodies for the indicated times in minutes. Data are representative of three independent experiments.

(E) Western blotting for pY and TCRζ in TCRζ IPs from purified CD4^{+} LN cells from either WT or LAT-Y136F mice stimulated with 10 μg/mL soluble anti-CD3ε antibodies for the indicated times in minutes, representative data from two independent experiments (left); and histogram of anti-CD3ε (above) or anti-TCRβ (below) staining in gated, CD4^{+} lymphocytes from 8-week-old WT versus LAT-Y136F mice.
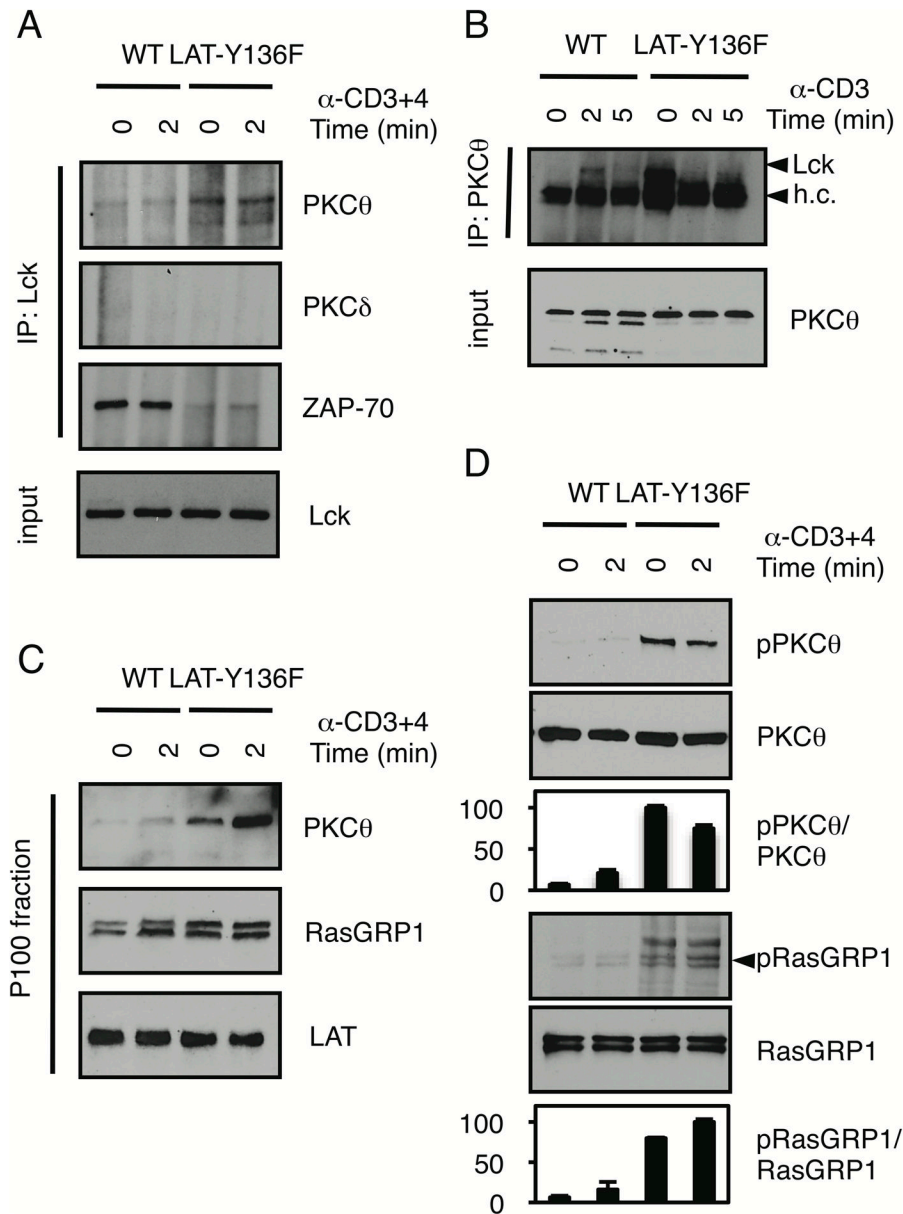
FIGURE 7. Enhanced Lck/PKCθ association and RasGRP1 membrane localization in CD4^{+} T lymphocytes isolated from LAT-Y136F mice

(A) Western blotting for PKCθ, PKCδ, and ZAP70 in Lck IPs and total Lck in WCL from purified CD4^{+} LN cells from either WT or LAT-Y136F mice stimulated with 10μg/mL soluble anti-CD3ε antibodies for the indicated times in minutes. Data are representative of three independent experiments.

(B) Western blotting for Lck in PKCθ IPs and total PKCθ in WCL from purified CD4^{+} LN cells from either WT or LAT-Y136F mice stimulated with 10 μg/mL soluble anti-CD3ε antibodies for the indicated times in minutes. h.c. denotes immunoglobulin heavy chain. Data are representative of three independent experiments.

(C) Western blotting for PKCθ, RasGRP1, and LAT in membrane (P100) fractions from purified CD4^{+} LN cells from either WT or LAT-Y136F mice stimulated with 10 μg/mL

soluble anti-CD3ε antibodies for the indicated times in minutes. Data are representative of two independent experiments.

(D) Western blotting for pPKCθ (T538), total PKCθ, pRasGRP1 (T184, doublet denoted by arrow) and total RasGRP1 (above, quantified below) in WCL from purified CD4$^+$ LN cells from either WT or LAT-Y136F mice stimulated with 10 μg/mL soluble anti-CD3ε + anti-CD4 antibodies for the indicated times in minutes. Data are representative of four independent experiments.
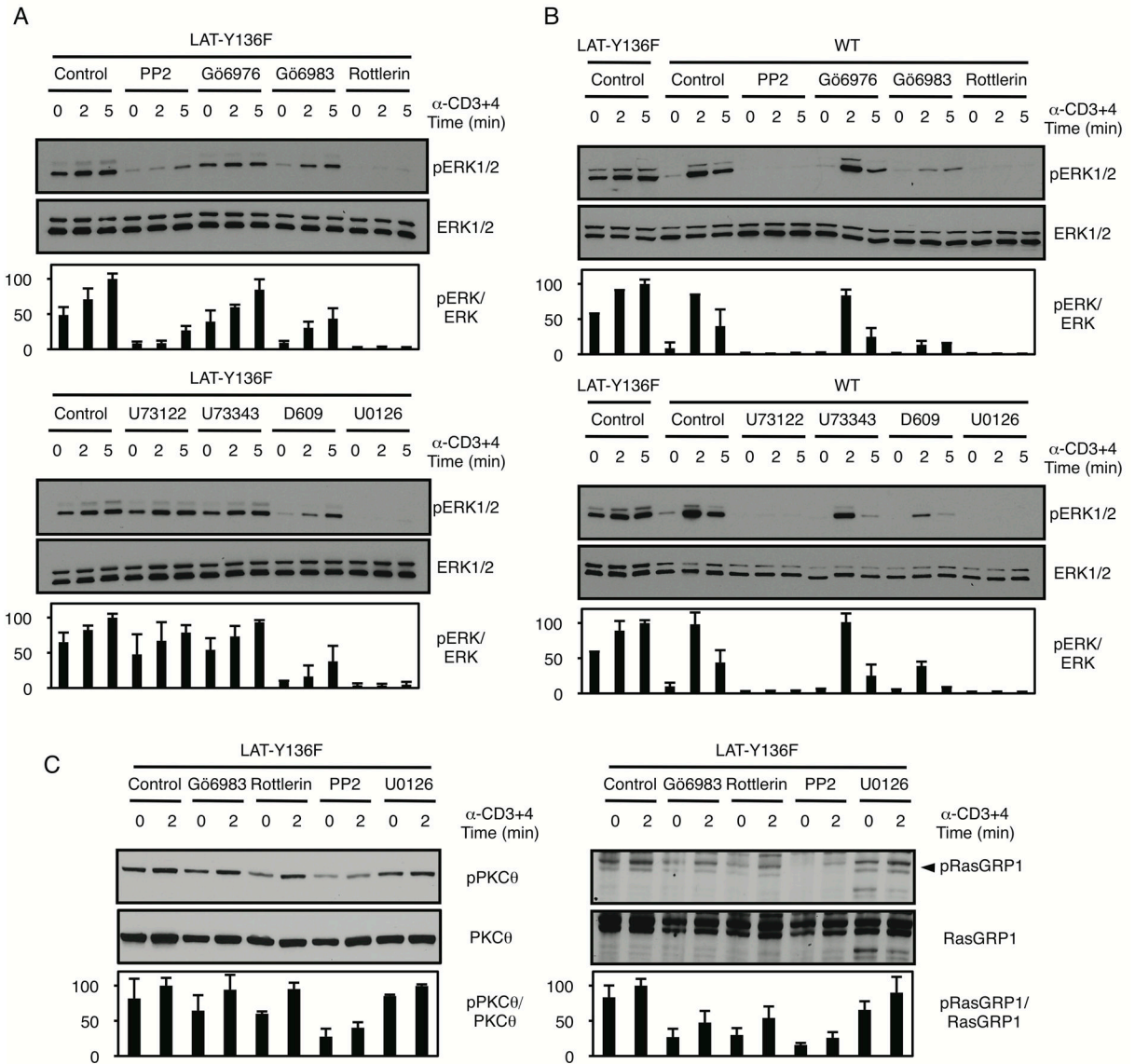
FIGURE 8. SFK and novel PKC signaling are required for ERK hyper-activation in CD4^{+} T lymphocytes isolated from LAT-Y136F mice

(A–B) Western blotting for phospho-ERK and total ERK (above, quantified below) in WCL from purified CD4^{+} LN cells from either LAT-Y136F (A) or WT (B) mice. Lysates were pre-treated with the indicated inhibitors and then stimulated with 10 μg/mL soluble anti-CD3ε + anti-CD4 antibodies. DMSO-treated cells represent the vehicle control, and MEK1/2 inhibition by U0126 is the positive control showing a complete loss of ERK phosphorylation. All stimulations were for the indicated times in minutes. Data are representative of three independent experiments.

(C) Western blotting for pPKCθ (T538), total PKCθ, pRasGRP1 (T184, doublet denoted by arrow), and total RasGRP1 (above, quantified below) in WCL from purified CD4^{+} LN cells from LAT-Y136F mice. Lysates were pre-treated with the indicated inhibitors and then stimulated with 10 μg/mL soluble anti-CD3ε + anti-CD4 antibodies. DMSO-treated cells represent the vehicle control. All stimulations were for the indicated times in minutes. Data are representative of two independent experiments.